The Physical Mechanism of Calcium Pump Regulation in the Heart

John Voss, Larry R. Jones, and David D. Thomas
Department of Biochemistry, University of Minnesota Medical School, Minneapolis, Minnesota 55455, and Department of Medicine, Krannert Institute of Cardiology, Indiana University School of Medicine, Indianapolis, Indiana 46202 USA

ABSTRACT The Ca-ATPase in the cardiac sarcoplasmic reticulum membrane is regulated by an amphipathic transmembrane protein, phospholamban. We have used time-resolved phosphorescence anisotropy to detect the microsecond rotational dynamics, and thereby the self-association, of the Ca-ATPase as a function of phospholamban phosphorylation and physiologically relevant calcium levels. The phosphorylation of phospholamban increases the rotational mobility of the Ca-ATPase in the sarcoplasmic reticulum bilayer, due to a decrease in large-scale protein association, with a $[Ca^{2+}]$ dependence parallel to that of enzyme activation. These results support a model in which phospholamban phosphorylation or calcium free the enzyme from a kinetically unfavorable associated state.

INTRODUCTION

Because of their complexity, most studies of biological membranes have focused on the characterization of individual components. However, a full understanding of membrane function requires the study of how membrane proteins interact with one another to establish a functional system. The modulation of the Ca-ATPase in cardiac sarcoplasmic reticulum (SR) by phospholamban (PLB) presents an interesting model for the study of such interactions. The Ca-ATPase relaxes muscle by coupling ATP hydrolysis to the transport of two Ca^{2+} ions across the SR membrane (Inesi et al., 1980). PLB (Tada and Katz, 1982; Simmerman et al., 1986), an integral membrane protein present in cardiac but not skeletal fast-twitch muscle, inhibits the Ca-ATPase at sub-micromolar ionized calcium but has little or no effect at or above micromolar Ca^{2+}. β-Adrenergic-induced phosphorylation of PLB relieves this inhibition. It has been proposed that a physical interaction between the protein and the Ca-ATPase is altered upon PLB phosphorylation – thereby relieving an inhibitory influence (James et al., 1989).

Our efforts to test this hypothesis have been stimulated by our studies of molecular dynamics and interactions in skeletal SR, in which the Ca-ATPase is highly homologous to the cardiac enzyme, but PLB is not present so the pump is not regulated. Using EPR and phosphorescence spectroscopies, we showed that Ca-ATPase enzymatic activity is quite sensitive to protein-protein interactions in skeletal SR, with decreased protein rotational mobility (due to increased Ca-ATPase association) correlating with decreased enzyme activity (Squier and Thomas, 1988; Squier et al., 1988a,b; Birmachu and Thomas, 1990; reviewed by Thomas and Mahaney, 1993, and by Thomas and Karon, 1993). In particular, the inhibition of the Ca-ATPase by melittin, a basic amphipathic peptide that is structurally related to PLB, is due primarily to the electrostatically induced aggregation of the Ca-ATPase in the plane of the SR membrane (Mahaney and Thomas, 1991; Voss et al., 1991). We subsequently found that the rotational mobility of the Ca-ATPase in cardiac SR is greatly reduced in relation to the enzyme in skeletal SR, due to large-scale aggregation of the enzyme in the plane of the membrane, and we proposed that this is due to the presence of unphosphorylated (inhibitory) PLB in this system (Birmachu et al., 1993). The key technique in this study was time-resolved phosphorescence anisotropy (TPA), which provides quantitative information about the rotational mobilities and mole fractions of different oligomeric species in the membrane (Birmachu and Thomas, 1990).

In the present study, to correlate more precisely the function and rotational dynamics of the cardiac Ca-ATPase, we report the effects of PLB phosphorylation on the rotational dynamics and association state of the enzyme, as measured by TPA, and we compare quantitatively the effects on enzyme function. Based on the results, we propose a model for the physical mechanism of Ca pump regulation in the heart.

MATERIALS AND METHODS

SR vesicle isolation

Dog cardiac SR membrane vesicles, containing both junctional and tubular SR, were isolated according to Jones and Cala (1981). Briefly, dog left ventricular tissue (~190 g) was homogenized three times for 30 s in 10 mM $NaHCO_3$ with a Polytron. SR vesicles were collected as the membranes sedimenting at 45,000 × *g* for 30 min. After extraction with 0.6 M KCl, 30 mM histidine, pH 7.0, the vesicles were pelleted by centrifugation at 45,000 × *g* for 30 min and resuspended in 0.25 M sucrose, 30 mM histidine, pH 7.2. The vesicles were frozen in small aliquots and stored at −40°C. Vesicles stored in this manner were stable indefinitely. Protein concentrations were determined by the biuret method (Gornall et al., 1949), using bovine serum albumin as a standard.

Ca uptake assay

To obtain accurate measurements of initial Ca uptake rates at submicromolar free calcium, we devised a spectrophotometric assay involving the chromophoric calcium chelator DFBAPTA, the 5-5′-difluoro derivative

Received for publication 29 September 1993 and in final form 27 April 1994.
Address reprint requests to Dr. David D. Thomas, Department of Biochemistry, Millard 4–225, University of Minnesota Medical School, Minneapolis, MN 55455. Tel.: 612-625-0957; Fax: 612-624-0632; E-mail: ddt@ddt.biochem.umn.edu.

0006-3495/94/07/190/07 $2.00

of 1,2-bis(*o*-aminophenoxy)ethane-*N, N,N',N'*-tetraacetic acid (Molecular Probes). Oxalate-facilitated Ca uptake rates were determined from the decrease in $[Ca]_T$, the total extravesicular calcium concentration, using a Hewlett Packard 8452A diode array spectrophotometer at pH 7.0 (25°C) in a stirred cuvette containing 60 mM KCl, 1 mM $MgCl_2$, 10 mM EGTA, 50 mM MOPS, 5 mM potassium oxalate, 1 mM Mg·ATP, 0.05–0.1 mg SR protein/ml, and 200 μM DFBAPTA. A variable amount of $CaCl_2$ was added to give the desired extravesicular free ionized calcium level ($[Ca^{2+}]$, designated below as $[Ca]$), as calculated with the computer program of Fabiato (1988). This same program was used to calculate the apparent calcium·EGTA association constant K_E,

$$K_E = \frac{[Ca \cdot EGTA]}{[Ca][EGTA]} \quad (1)$$

which is a function of all association constants for each ligand in the solution, the temperature, and the pH.

As calcium is pumped into the SR vesicle, the total calcium concentration ($[Ca]_T$) in the extra-vesicular solution decreases. The $[Ca]_T$ can be related to the $[Ca]$ (free ionized Ca^{2+}) by the following expression:

$$[Ca]_T = [Ca]\left(1 + \frac{K_E[EGTA]_T}{1 + K_E[Ca]}\right) \quad (2)$$

Thus, a detected change in extravesicular $[Ca]$ can be converted with K_E into a change in the total calcium level $[Ca]_T$ in the extravesicular medium. Calcium pumped into the SR directly depletes this total calcium level. The rate of decrease of $[Ca]_T$, divided by the amount of protein, is the desired specific calcium uptake activity. So all we need is a measurement of extravesicular $[Ca]$. This is provided by the absorbance of DFBAPTA, which has an extinction coefficient ϵ_B (302 nm) of ~4000 cm^{-1} M^{-1} in the calcium-free state (BAP) and 0 in the calcium-bound state (Ca·BAP) (Pethig et al., 1989; Tsien, 1980). An accurate value of ϵ_B was obtained by measuring the absorbance of standard DFBAPTA solutions under our assay conditions. The absorbance at 302 nm can then be used to calculate [Ca] according to

$$[Ca] = \frac{1}{K_B}\left(\frac{[BAP]_T}{[BAP]} - 1\right) \quad (3)$$

where $K_B = [Ca{\cdot}BAP]/[Ca][BAP]$, the apparent association constant for calcium and DFBAPTA, and $[BAP]_T = [BAP] + [Ca{\cdot}BAP]$. K_B was determined under our assay conditions by measuring A(302 nm), thus yielding $[BAP] = A(302\text{ nm})/\epsilon_B$, for a series of calcium standards (prepared using the Fabiato program) at a set $[BAP]_T$, and fitting the results to Eq. 3.

Time-dependent absorbance spectra were acquired using the spectrophotometer's internal software. Further data processing was done with a computer program (available upon request) written by Nicoleta Cornea, which performed the following calculations on each time point: 1) The effect of increased light scattering due to the accumulation of Ca oxalate was corrected according to $A_{302} = OD_{302} - OD_{346}\cdot(346/302)^{3.8}$. 2) $[Ca]$, the concentration of free ionized calcium, was calculated using Eq. 3, where $[BAP] = \epsilon_B/A_{302}$, $\epsilon_B = 3938$ cm^{-1} M^{-1}, and $K_B = 6.8 \times 10^6$ M^{-1}. (3) $[Ca]_T$, the total extravesicular calcium concentration, was calculated using Eq. 2, where $K_E = 2.5 \times 10^6$ cm^{-1} M^{-1}.

Fig. 1 demonstrates the DFBAPTA absorbance change and the corresponding calculated change in total extravesicular calcium $[Ca]_T$. The initial rate of change of $[Ca]_T$ (slope of Fig. 1, determined from a linear least-squares fit to the initial linear time range) was divided by the protein concentration to obtain the specific calcium uptake activity. This method of Ca uptake measurement allows for true initial velocity determination, resulting in transport values higher than typically reported using filtration assays over several minutes (Chamberlain et al., 1983). The Ca uptake values we obtained by this assay agree well with the Ca-ATPase rates measured for the same preparations, assuming a coupling ratio of two Ca transported per ATP hydrolyzed.

Phosphorylation

Phospholamban phosphorylation was performed just before TPA data collection by splitting the sample in half to incubate with or without 40 μg/ml of the catalytic subunit of protein kinase A in a buffer containing 50 mM Tris-HCl, 0.1 mM dithiothreitol, 2 mM $MgCl_2$, 0.75 mM ATP containing 2–3 mCi/ml [γ-^{32}P]ATP, 50 nM phosphatase inhibitor calyculin A (LC Laboratories), pH 7.0 at 30°C. After a 3-min incubation, the sample was immediately centrifuged at 100,000 × *g* for 5 min. The control and phosphorylated SR vesicles were then suspended in 30 mM MOPS, 250 mM sucrose, 50 nM calyculin A, pH 7.0, and kept on ice.

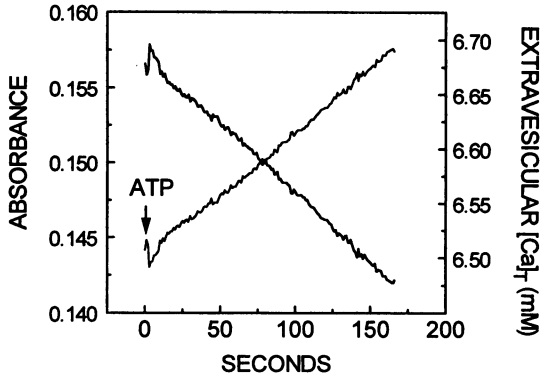

FIGURE 1 Change in DFBAPTA absorbance at 302 nm (*solid line*) with corresponding change in the calculated total extravesicular calcium concentration (*broken line*) of dog cardiac SR at 0.3 μM ionized calcium (see Materials and Methods).

ERITC labeling

For phosphorescence experiments, the Ca-ATPase in SR vesicles was specifically labeled on lysine 515 with ERITC as described previously (Birmachu and Thomas, 1990). This procedure results in specifically labeling of Lys 515 on the Ca-ATPase in both skeletal and cardiac SR (Birmachu et al., 1993). ERITC labeling of this residue results in enzyme inactivation, probably due to the label's occupation of the nucleotide binding site (Birmachu and Thomas, 1990). Extensive studies with skeletal SR labeled at the same site with a very similar probe (fluorescein isothiocyanate) show that the enzyme is otherwise unperturbed, has normal calcium binding, and goes through the normal calcium-pumping enzymatic cycle with less bulky substrates such as acetyl phosphate (Teruel and Inesi, 1988). It has also been shown that the enzyme's rotational dynamics are not affected by ATP binding (Lewis and Thomas, 1991). Therefore, the rotational dynamics of ERITC-SR are probably representative of the unlabeled protein. Labeled samples were kept on ice and used the same day for spectroscopic measurements.

SDS gels and autoradiography

Sodium dodecyl sulfate (SDS)-polyacrylamide gel electrophoresis was performed according to the method of Jones et al. (1985) using an 8% slab gel, 1.5 mm thick. As described previously (Birmachu et al., 1993), specificity of stoichiometric ERITC labeling to Lys 515 was confirmed by quantitative analysis of fluorescent photographs of SDS gels taken through a 550 nm cut-off filter using a UV lamp before staining the gels with Coomassie blue. The Coomassie blue-stained gels and the fluorescence negatives were scanned with a densitometer (Hoefer Scientific Instruments) to quantitate the amount of protein and label, respectively. The Ca-ATPase comprised 36 ± 3% and 79 ± 2% of the total detected protein in dog cardiac and rabbit skeletal SR preparations, respectively. As demonstrated previously, 90–95% of the ERITC fluorescence was localized to the 110-kDa Ca-ATPase band in SDS gels of both dog cardiac and rabbit skeletal SR (Birmachu et al., 1993).

Specificity of phospholamban phosphorylation was measured from aliquots taken directly from assay and spectroscopy samples, combined 1:1 with gel dissociation medium (60 mM Tris, 15% SDS, 20% glycerol, 0.1%

bromphenol blue) and placed on dry ice. A total of 10–15 μg SR protein were loaded per lane onto an 8% SDS-PAGE gel, 1.5 mm thick. The gels were then dried and placed in an 8 × 10 inch x-ray developing cassette containing Kodak X-OMAT XAR-5 film and a DuPont Cronex intensifying screen. Regions on the gel corresponding to the exposed regions on the developed film were cut and scintillation counted, corrected for background, and compared against the total counts using 10 μl of the ATP cocktail diluted to 0.5 mM. Fig. 2 illustrates highly specific phosphorylation by the protein kinase A catalytic subunit (Sigma Chemical Co., St. Louis, MO) of phospholamban in dog cardiac SR. Following TPA data collection on a sample, four separate measurements of phosphorylation at phospholamban, in three different dog cardiac SR preparations, resulted in an average of 0.98 ± 0.05 nmol phosphate per mg SR protein. Under these conditions, all detectable phosphorylation was localized to the phospholamban protein. While slightly higher levels of phospholamban phosphorylation were obtainable with prolonged protein kinase incubation times, such conditions resulted in a loss of phosphorylation specificity and no further effect on Ca uptake activity (discussed below).

To ensure that no significant dephosphorylation (by the endogenous SR phosphatases) of phospholamban occurred on the time course of the experiments, dog cardiac SR vesicles (0.5 mg) were phosphorylated as described above, centrifuged, and resuspended in 250 mM sucrose, 30 mM MOPS, 50 nM calyculin A, pH 7.0. The phosphorylated SR was then transferred to the standard experiment solution (50 mM MOPS, 60 mM KCl, 1 mM $MgCl_2$, 10 mM EGTA, 5 mM $CaCl_2$, 50 nM calyculin A, pH 7.0) to a concentration of 0.4 mg/ml and incubated at 25°C. At time points of 5, 15, 30, 60, and 90 min, a 50-μl aliquot of the phosphorylated SR suspension was combined with 30 μl of the gel dissociation medium (see above) and immediately frozen on dry ice. 70 μl (0.02 mg) of the thawed samples were then loaded onto an 8% SDS-PAGE gel and electrophoresed for 6 h. The protein concentration of each aliquot was assayed using the BCA Protein Kit (Pierce Chemical) and the gel autoradiographed. Fig. 3 shows the exposed x-ray film of a typical stability experiment. Dephosphorylation of phospholamban never exceeded 10% over 30 min at 25°C, indicating that spectroscopy measurements (discussed below) were completed before significant dephosphorylation.

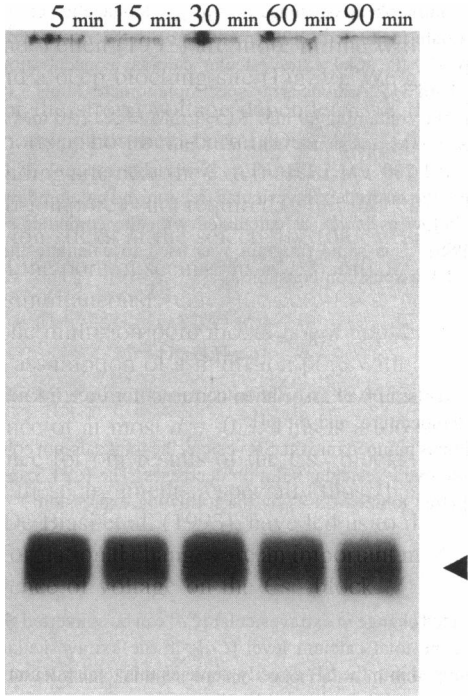

FIGURE 3 Stability of phospholamban phosphorylation. Shown is an autoradiogram of dog cardiac SR incubated at 25°C for 5 (*lane 1*), 15 (*lane 2*), 30 (*lane 3*), 60 (*lane 4*), and 90 min (*lane 5*) following phosphorylation with [γ-^{32}P]ATP. The phosphate content at the phospholamban band, indicated by arrow, was 0.94, 0.93, 0.91, 0.77, and 0.74 nmol phosphate per mg SR protein for *lanes 1–5,* respectively.

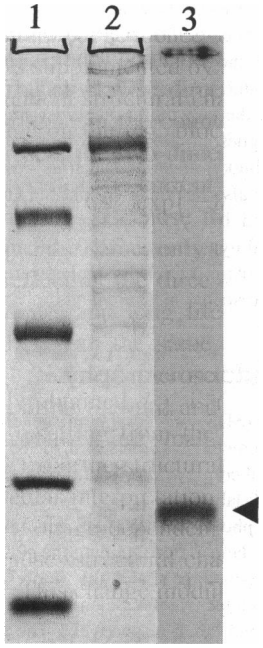

FIGURE 2 Autoradiogram of ^{32}P-phosphorylated phospholamban (*arrow, lane 3*). *Lanes 1* and *2* show the Coomassie blue-stained protein bands of molecular weight standards and dog cardiac SR on a SDS-PAGE gel, respectively. The molecular weight standards are, from top to bottom, phosphorylase B (97.4 kDa), bovine serum albumin (66.2 kDa), ovalbumin (45 kDa), carbonic anhydrase (31 kDa), and soybean trypsin inhibitor (21.5 kDa).

Time-resolved phosphorescence anisotropy

The experimental and analytical procedures for TPA of skeletal and cardiac SR have been described in detail previously (Birmachu et al., 1993). Phosphorescence experiments were carried out in a solution containing 60 mM KCl, 1 mM $MgCl_2$, 10 mM EGTA, 50 mM MOPS, and an amount of $CaCl_2$ resulting in the desired ionized calcium level (Fabiato, 1988), pH 7.0 (25°C). Before TPA data collection, oxygen was enzymatically removed from the sample (0.2- 0.4 mg/ml) in a sealed 1- cm quartz cuvette with 100 μg/ml glucose oxidase, 15 μg/ml catalase, and 5 mg/ml glucose for 10–15 min, as described previously (Birmachu et al., 1993). The spectrometer used to obtain TPA decays was described previously (Ludescher and Thomas, 1988). The phosphorescence anisotropy (r) is given by

$$r = \frac{I_\parallel - GI_\perp}{I_\parallel + 2GI_\perp} \tag{4}$$

where $I_\parallel$ and $I_\perp$ are the time-dependent decays of the phosphorescence intensities observed through polarizers oriented parallel and perpendicular, respectively, to the vertically polarized excitation pulse. G is an instrumental correction factor determined from the apparent anisotropy of the free dye in solution, for which the corrected anisotropy is 0. TPA decays of ERITC-labeled Ca-ATPase were detected and signal-averaged for 20 loops, each consisting of 2000 acquisitions of $I_\parallel(t)$ and 2000 acquisitions of $I_\perp(t)$. The laser repetition rate was 100–200 Hz, so a typical experiment lasted about 10 min.

TPA decays were analyzed as reported previously (Birmachu and Thomas, 1990), using a nonlinear least-squares fit to a sum of exponentials

plus a constant:

$$A(t) = \sum_{i=1}^{n} A_i e^{-t/\phi_i} + A_\infty \quad (5)$$

where ϕ_i are rotational correlation times, A_i are the normalized amplitudes (r_i/r_0), A_∞ is the normalized residual anisotropy (r_∞/r_0), and r_0 is the initial anisotropy ($r(0) = r_0 = \Sigma r_i + r_\infty$). The goodness-of-fit for the anisotropy decays was evaluated by comparing χ^2 values for the multiexponential fits, and by comparing plots of the residuals (the difference between the measured and the calculated values).

It has been shown previously (Birmachu and Thomas, 1990) that the TPA of ERITC-SR is dominated by the uniaxial rotation of the labeled Ca-ATPase about an axis normal to the bilayer. For this model, each different rotational diffusion coefficient should give rise to a biexponential decay component (Kinosita et al., 1984; reviewed by Thomas, 1986), but it has been shown that a single-exponential approximation is sufficient to describe the decay for each rotating species in ERITC-SR (Birmachu and Thomas, 1990). Then, as long as the probe orientation relative to the protein is the same for all proteins, the mole fraction (f_i) of probes in the ith rotating species, having rotational correlation time ϕ_i is given by

$$f_i = A_i/(1 - A_{\infty o}), \quad f_I = (A_\infty - A_{\infty o})/(1 - A_{\infty o}) \quad (6)$$

where f_I is the fraction of probes (proteins) that are immobile on the time scale of the experiment (Birmachu et al., 1993). $A_{\infty o}$ is the residual anisotropy of a reference sample for which $f_I = 0$ and describes the extent to which the probe's motion is restricted in angular range, due to the fixed angles θ_{ma}, and θ_{me} of the probe's absorption and emissions transition moments relative to the membrane normal:

$$A_{\infty o} = \frac{P_2(\cos^2\theta_{ma})P_2(\cos^2\theta_{me})}{P_2(\cos^2\theta_{ae})} \quad (7)$$

where $P_2(x) = (3x^2 - 1)/2$, and θ_{ae} is the angle between the absorption and emission transition moments (Lipari and Szabo, 1980). $A_{\infty o}$ has been shown to be 0.22 for ERITC-Ca-ATPase in skeletal SR (Birmachu and Thomas, 1990), and is assumed to be the same for cardiac SR (Birmachu et al., 1993).

The rotational diffusion coefficient (D_m) for uniaxial rotation of a cylindrical membrane protein can be expressed as a function of the membrane lipid viscosity (η), the temperature (T), and the effective radius (a) of the portion of the protein in the bilayer (Saffman and Delbrück, 1975):

$$D_m = \frac{kT}{4\pi a^2 h\eta} \propto \frac{1}{\phi} \quad (8)$$

where h is the thickness of the hydrocarbon phase of the lipid bilayer. Thus, the rotational correlation time (inversely proportional to the diffusion coefficient), should be proportional to the lipid viscosity (inverse of fluidity) and to the intramembrane cross-sectional area (πa^2) of the rotating protein. This theory relating protein size and lipid fluidity to protein rotational mobility is supported by previous studies on the Ca-ATPase as measured by both ST-EPR (Squier et al., 1988a,b) and phosphorescence anisotropy (Birmachu and Thomas, 1990). The lipid viscosity η is essentially the same in skeletal and cardiac SR (Birmachu et al., 1993), so PLB has no significant effect on lipid viscosity. Therefore, any PLB-dependent changes in the observed rotational correlation times must be due to changes in the effective radius (a in Eq. 8) of the rotating protein. The only plausible source of large changes in protein size in SR is protein association into different sized oligomers, with the rotational correlation time ϕ_i roughly proportional to the size of the oligomer (Birmachu and Thomas, 1990). Thus the distribution of oligomeric species is given by the fractions f_i (Eq 6). The fraction of proteins in immobile species f_I, determined from the residual anisotropy A_∞, thus corresponds to protein aggregates so large that they undergo little or no rotational diffusion in the 1 ms time window of the TPA experiment. Since the correlation time of a Ca-ATPase monomer or dimer is on the order of 10–20 μs, these immobile aggregates must contain more than 10 Ca-ATPase molecules (Birmachu and Thomas, 1990; Voss et al., 1991; Birmachu et al., 1993).

RESULTS AND DISCUSSION

Effects of PLB phosphorylation on calcium uptake

PLB phosphorylation at Ser-16, by cAMP-dependent protein kinase, stimulates sarcoplasmic reticulum (SR) Ca uptake up to fourfold, depending on the calcium level (Fig. 4), in agreement with previous studies (Tada and Katz, 1982). Following PLB phosphorylation, the K_m (Ca^{2+}) for the enzyme in cardiac SR is decreased by 0.3 pCa units, to a value similar to that of the PLB-devoid fast-twitch skeletal SR (see legend to Fig. 4). In accordance with this, MacLennan and co-workers have shown that the fast-twitch and cardiac isoforms of the Ca-ATPase expressed in COS cells are indistinguishable with respect to calcium activation, and that co-expression of PLB with either isoform depresses the Ca^{2+} affinity to a level similar to that of the enzyme in native, nonphosphorylated cardiac SR (Toyofuku et al., 1989).

Effects of PLB phosphorylation on Ca-ATPase rotational dynamics

PLB phosphorylation has a substantial effect on the TPA decay of phosphorescent-labeled cardiac Ca-ATPase at 0.3 μM Ca^{2+} (Fig. 5). Phosphorylation clearly lowers the final (residual) anisotropy ($A_\infty = r_\infty/r_0$), implying increased rotational mobility, intermediate between those of unphosphorylated cardiac and fast-twitch SR, which lacks PLB. TPA decays were analyzed to determine the rotational correlation

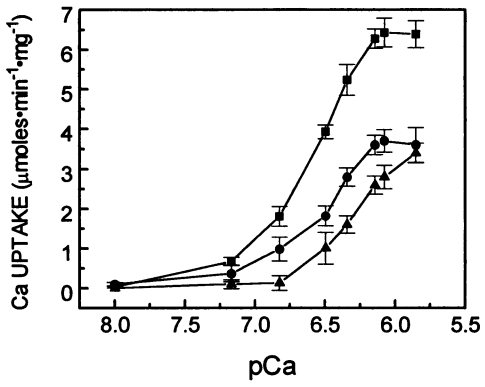

FIGURE 4 Ca uptake of sarcoplasmic reticulum vesicles from rabbit skeletal fast-twitch (■), and phosphorylated (●) and control (▲) dog cardiac muscle (0.1 mg/ml) in a buffer containing 50 mM MOPS, 60 mM KCl, 2 mM $MgCl_2$, 10 mM potassium oxalate, 5 mM sodium azide, 1 mM ATP, 10 mM EGTA, pH 7.0, 25°C, and an amount of $CaCl_2$ to give the desired free [Ca^{2+}]. The higher V_{max} of skeletal SR is due to the twofold greater enrichment of the Ca-ATPase in this preparation (Birmachu et al., 1993). A fit of the data to

$$v = (V_{MAX}S^n)/(K_{0.5}^n + S^n)$$

gave $K_{0.5}$ and V_{max} values of 0.52 μM and 3.79 μmol·min^{-1}·mg^{-1}; 0.27 μM and 3.8 μmol·min^{-1}·mg^{-1}; 0.27 μM and 7.1 μmoles·min^{-1}·mg^{-1}; for cardiac control, cardiac phosphorylated, and fast-twitch skeletal SR respectively, with $n = 2 \pm 0.15$ for each fit. Error bars represent the standard deviations from three experiments.

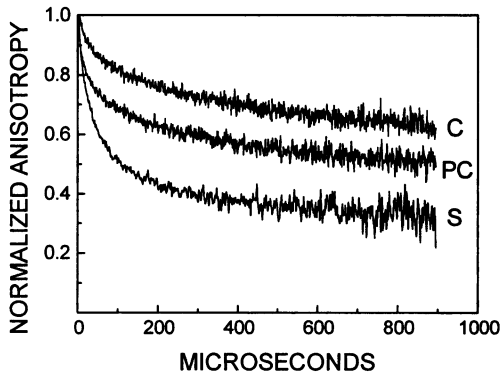

FIGURE 5 Time-resolved phosphorescence anisotropy decays of control cardiac (C), phosphorylated cardiac (PC), and fast-twitch skeletal (S) SR vesicles (0.3–0.6 mg/ml) at 25°C in 50 mM MOPS, 60 mM KCl, 1 mM $MgCl_2$, 10 mM EGTA, 4.24 mM $CaCl_2$, pH 7.0, with a free $[Ca^{2+}]$ of 0.3 μM.

times and mole fractions of the various sizes of protein aggregates in the membrane (Birmachu and Thomas, 1990; Voss et al., 1991; Birmachu et al., 1993). The fits to multiexponential decays (Eq. 5, Table 1) show little or no significant variation in the correlation times ϕ_i, but there are substantial changes in the pre-exponential factors A_i, consistent with a redistribution of Ca-ATPase molecules among the populations corresponding to different oligomeric species. The most significant effect of phosphorylation is a decrease in A_∞, corresponding to a decrease in the fraction of Ca-ATPase molecules immobilized in large aggregates (f_1 in Eq. 6), whose motion is too slow to detect on the 1-ms TPA time scale (Birmachu and Thomas, 1990; Voss et al., 1991; Birmachu et al., 1993). Table 1 shows that this decrease in A_∞ is accompanied by a slight decrease in A_3, corresponding to a decrease in the mole fraction of large but mobile oligomers (f_3 in Eq. 6), and substantial increases in A_1 and A_2, corresponding to an increase in the mole fraction of monomers and smaller oligomers (f_1 and f_2 in Eq. 6).

The anisotropy decays do not decay completely to a constant value during the time window of observation (Fig. 5), so the extrapolated values for A_∞ obtained from fits may have systematic errors not included in the statistical uncertainties given in Table 1. Nevertheless, the relative A_∞ values for the different samples, on which most of our conclusions are based, are probably reliable, since they did not depend significantly on the time window included in the fit. As discussed in METHODS, A_∞ changes can be due to either changes in large-scale aggregation (f_1 in Eq. 6), as assumed here, or in probe orientation relative to the membrane normal (Eq. 7). We cannot rule out completely the possibility that PLB (or PLB phosphorylation) causes a protein conformational change on the Ca-ATPase that results in a change in probe orientation without a change in the protein's rotational mobility. However, previous TPA and EPR studies on both skeletal and cardiac SR indicate that immobilization due to aggregation is a much more likely explanation (Birmachu and Thomas, 1990; Voss et al., 1991; Birmachu et al., 1993). For example, both TPA and EPR, with probes attached to different sites, show that the Ca-ATPase is less mobile in cardiac than in skeletal SR (Birmachu et al., 1993).

The $[Ca^{2+}]$-dependent effect of PLB phosphorylation on large-scale enzyme aggregation (Fig. 6) closely parallels the effect on enzymatic activity (Fig. 4), supporting our hypothesis that Ca-ATPase mobility can predict the functional state of the enzyme. PLB phosphorylation has its largest effect on both enzyme mobilization (disaggregation) and activation at low (sub-micromolar) Ca^{2+}, while having negligible effects on both at micromolar Ca^{2+}. These results appear to contradict a previous report (Fowler et al., 1989) of slightly decreased Ca-ATPase mobility following phosphorylation, but that study was performed at functionally irrelevant $[Ca^{2+}]$,

TABLE 1 Effect of PLB phosphorylation and Ca^{2+} on TPA parameters of ERITC-labeled Ca-ATPase in cardiac SR

PLB	$[Ca^{2+}]$ (μM)	ϕ_1 (μs)	ϕ_2 (μs)	ϕ_3 (μs)	A_1	A_2	A_3	A_∞	r_0
Unphosphorylated									
	0.01	12 ± 3	100 ± 35	287 ± 80	0.072 ± 0.014	0.081 ± 0.022	0.112 ± 0.029	0.737 ± 0.013	0.089 ± 0.002
	0.05	14 ± 4	112 ± 23	290 ± 66	0.087 ± 0.008	0.119 ± 0.009	0.094 ± 0.013	0.700 ± 0.018	0.088 ± 0.003
	0.10	8 ± 1	85 ± 17	285 ± 78	0.106 ± 0.014	0.101 ± 0.011	0.109 ± 0.023	0.684 ± 0.020	0.090 ± 0.003
	0.30	11 ± 3	103 ± 11	383 ± 130	0.104 ± 0.017	0.128 ± 0.022	0.103 ± 0.024	0.665 ± 0.010	0.096 ± 0.005
	0.50	10 ± 1	115 ± 10	427 ± 109	0.099 ± 0.011	0.128 ± 0.020	0.127 ± 0.016	0.642 ± 0.014	0.086 ± 0.002
	0.76	9 ± 1	65 ± 13	272 ± 94	0.112 ± 0.022	0.144 ± 0.023	0.132 ± 0.024	0.612 ± 0.006	0.093 ± 0.007
	1.00	7 ± 1	55 ± 12	385 ± 85	0.098 ± 0.015	0.155 ± 0.010	0.159 ± 0.015	0.594 ± 0.006	0.086 ± 0.002
	1.60	7 ± 2	61 ± 14	408 ± 129	0.128 ± 0.010	0.192 ± 0.012	0.177 ± 0.005	0.497 ± 0.024	0.094 ± 0.005
Phosphorylated									
	0.01	8 ± 1	72 ± 10	435 ± 47	0.115 ± 0.012	0.116 ± 0.023	0.193 ± 0.014	0.575 ± 0.003	0.101 ± 0.007
	0.05	10 ± 3	93 ± 20	580 ± 71	0.112 ± 0.022	0.143 ± 0.016	0.196 ± 0.013	0.549 ± 0.006	0.094 ± 0.008
	0.10	7 ± 1	73 ± 22	460 ± 118	0.105 ± 0.016	0.145 ± 0.011	0.218 ± 0.008	0.531 ± 0.004	0.092 ± 0.007
	0.30	11 ± 3	68 ± 19	323 ± 101	0.142 ± 0.008	0.154 ± 0.023	0.191 ± 0.003	0.514 ± 0.004	0.095 ± 0.003
	0.50	6 ± 1	55 ± 12	385 ± 88	0.138 ± 0.011	0.160 ± 0.012	0.201 ± 0.018	0.502 ± 0.007	0.091 ± 0.005
	0.76	7 ± 1	55 ± 10	320 ± 64	0.135 ± 0.024	0.181 ± 0.011	0.199 ± 0.016	0.486 ± 0.008	0.092 ± 0.004
	1.0	7 ± 1	73 ± 20	480 ± 56	0.143 ± 0.010	0.196 ± 0.007	0.197 ± 0.009	0.465 ± 0.010	0.088 ± 0.002
	1.60	8 ± 1	63 ± 11	435 ± 75	0.152 ± 0.015	0.183 ± 0.019	0.176 ± 0.011	0.489 ± 0.020	0.093 ± 0.003

TPA decays were fit to Eq. 5 as described in Materials and Methods. Three exponentials ($n = 3$ in Eq. 5) were found to give optimal fits, based on χ^2 values and plots of the residuals (the difference between the measured and the calculated values). Each value in the table is the average from six experiments on separate preparations.

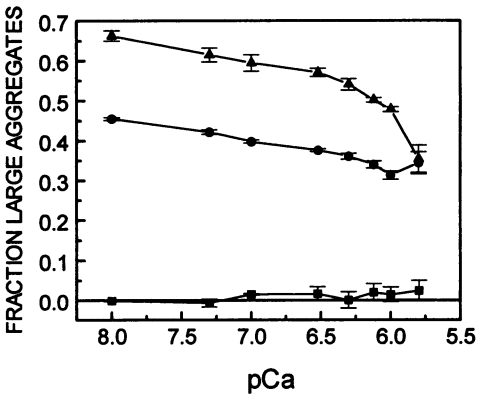

FIGURE 6 Fraction of Ca-ATPase molecules in large-scale aggregates as a function of [Ca^{2+}] in phosphorylated (●) and control (▲) cardiac SR, and in skeletal SR (■). This fraction was calculated as described previously (Birmachu et al., 1993) from $f_l = (A_\infty - 0.22)/(1 - 0.22)$ (Eq. 6), where the normalized residual anisotropy (A_∞, Table 1) was determined from a fit of the TPA data to Eq. 5.

the phosphorescence data were not analyzed quantitatively, and the experiments were flawed by a low specificity of PLB phosphorylation.

Effects of Ca^{2+} alone

The quantitative correlation between enzyme disaggregation and activation is further supported by the effect of Ca^{2+} in the absence of PLB phosphorylation. While phosphorylation has a substantial disaggregating effect at submicromolar [Ca^{2+}], micromolar Ca^{2+} itself induces enzyme disaggregation in unphosphorylated cardiac SR (Fig. 6, *triangles*), which parallels the activation of the pump (Fig. 4). No Ca^{2+} effect is observed on skeletal SR, which lacks PLB (Fig. 6, *squares*). This suggests that the physical PLB-enzyme interaction is mediated by calcium as well as phosphorylation, a conclusion consistent with the regulatory influence of PLB on the enzyme in the submicromolar Ca^{2+} range (Fig. 4). Thus PLB enhances the calcium dependence of enzyme activation in cardiac SR. Consistent with the physiological demands of the system, high (micromolar) calcium (where calcium transport rates must be accelerated) relieves PLB inhibition of Ca uptake, regardless of PLB's phosphorylation state.

Molecular model

PLB is a 52-residue, primarily α-helical peptide, which probably exists in the SR membrane as a pentamer due to a tightly interacting hydrophobic transmembrane domain (Simmerman et al., 1986). Phosphorylation of PLB results in neutralization of the basic residues clustered in the cytoplasmic domain of the protein, causing the pI to change from 11 to 7 (Jones et al., 1985). This charge reversal is key to the mechanism of PLB regulation, as evidenced by the electrostatic dependence of regulation (Xu and Kirchberger, 1989; Chiesi and Schwaller, 1989). Our model of PLB regulation, consistent with thermodynamic data on cardiac SR (Chiesi, 1979), involves the restriction of the Ca-ATPase in a kinetically unfavorable associated state that can be reversed by either calcium or phosphorylation (Fig. 7). It is possible that the basic residues of PLB interact with a regulatory calcium binding site on the Ca-ATPase. Inhibition by lanthanides, at cytoplasmic sites separate from the high-affinity Ca transport sites located in the transmembrane domain (Henao et al., 1992; Asturias and Blasie, 1991; Sprowl and Thomas, 1989), may involve the same residues. However, our observations can also be explained by a preferential interaction between PLB and the Ca-free (E2) conformation of the enzyme, as proposed previously (James et al., 1989; Toyofuku et al., 1989). Consistent with this hypothesis, we have found that PLB phosphorylation increases the tryptophan fluorescence of the Ca-ATPase, suggesting destabilization of E2 (unpublished observations).

A cross-linking study (James et al., 1989) has identified a PLB-interaction region C-terminal to the phosphorylation domain of the enzyme. Mutagenesis has confirmed that this region, along with the residues in the nucleotide-binding/hinge domain, must be conserved to maintain PLB regulation (Toyofuku et al., 1989). The structural characterization of this site is of particular interest, since several ion pumps of this class are affected by basic amphipathic peptides (Voss et al., 1991; Mahaney and Thomas, 1991; Cuppoletti et al., 1992; Raynor et al., 1991; Cuppoletti and Abbott, 1990; Vorherr et al., 1992). The mechanism proposed in Fig. 7, showing a structural and functional perturbation of an integral membrane protein through interaction with an amphipathic peptide that affects protein self-association, may be

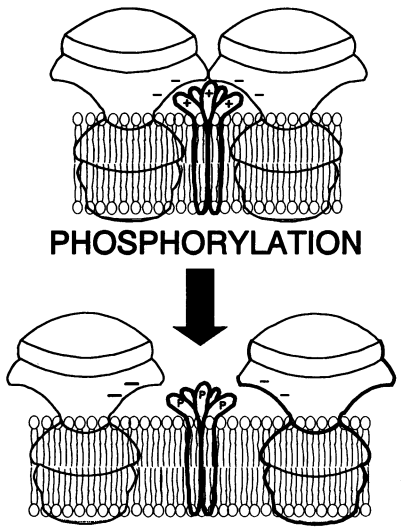

FIGURE 7 Model for the increased rotational mobility (decrease in large-scale aggregation) and relief of PLB-dependent inhibition of the Ca-ATPase, following PLB phosphorylation. Phosphorylation neutralizes the positive charge on the basic cytoplasmic portion of PLB, thereby disrupting the electrostatic interaction between PLB and one or more negative charge clusters on the cytoplasmic domain of the enzyme. A similar disaggregation is produced by micromolar Ca^{2+}. Only two Ca-ATPase molecules are shown, but large-scale aggregation, involving 10 or more Ca-ATPase molecules (as indicated by the TPA data) may be required for inhibition.

important in a wide range of membrane functions. Correlation of function with molecular dynamics, measured with site-directed spectroscopic probes, will be essential for further testing and refining this hypothesis.

We thank Nicoleta Cornea, Robert L. H. Bennett, and Franz L. Nisswandt for technical assistance.

This work was supported by a grant to D.D.T. from the American Heart Association, Minnesota Affiliate.

REFERENCES

Asturias, F., and J. K. Blasie. 1991. Location of high-affinity metal binding sites in the profile structure of the Ca^{2+} ATPase in the sarcoplasmic reticulum by resonance x-ray diffraction. *Biophys. J.* 59:488–502.

Birmachu, W., and D. D. Thomas. 1990. Rotational dynamics of the Ca-ATPase in sarcoplasmic reticulum studied by time-resolved phosphorescence anisotropy. *Biochemistry.* 29:3904–3914.

Birmachu, W., J. Voss, C. F. Louis, and D. D. Thomas. 1993. Protein and lipid rotational dynamics in cardiac and skeletal sarcoplasmic reticulum detected by EPR and phosphorescence anisotropy. *Biochemistry.* 32:9445–9453.

Chamberlain, B. K., D. O. Levitsky, and S. Fleischer. 1983. Isolation and characterization of canine cardiac sarcoplasmic reticulum with improved Ca^{2+} transport properties. *J. Biol. Chem.* 258:6602–6609.

Chiesi, M. 1979. Temperature-dependency of the functional activities of dog cardiac sarcoplasmic reticulum: a comparison with sarcoplasmic reticulum from rabbit and lobster muscle. *J. Mol. Cell. Cardiol.* 11:245–259.

Chiesi, M., and R. Schwaller. 1989. Involvement of electrostatic phenomena in phospholamban-induced stimulation of Ca uptake into cardiac sarcoplasmic reticulum. *FEBS Lett.* 244:241–244.

Cuppoletti, J., and A. J. Abbott. 1990. Interaction of melittin with the (Na^+ + K^+) ATPase: evidence for a melittin-induced conformational change. *Arch. Biochem. Biophys.* 283:249–257.

Cuppoletti, J., B. V. Chernyak, P. Huang, and D. H. Malinowska. 1992. Structure-function relationships in the interaction of amphipathic helical polypeptides with the gastric H/K ATPase. *Ann. N. Y. Acad. Sci.* 671: 443–445.

Fabiato, A. 1988. Computer programs for calculating total from specified free or free from specified total ionic concentrations in aqueous solutions containing multiple metals and ligands. *Methods Enzymol.* 157:378–417.

Fowler, C., J. Huggins, C. Hall, C. Restall, D. Chapman. 1989. The effects of calcium, temperature and phospholamban phosphorylation on the dynamics of calcium-stimulated ATPase of canine cardiac sarcoplasmic reticulum. *Biochim. Biophys. Acta.* 980:348–356.

Gornall, A., C. Bardawill, and M. David. 1949. Determination of serum proteins by means of the biuret reaction. *J. Biol. Chem.* 177:751–766.

Henao, F., S. Orlowski, Z. Merah, and P. Champeil. 1992. The metal sites on sarcoplasmic reticulum that bind lanthanide ions with the highest affinity are not the ATPase Ca^{2+} transport sites. *J. Biol. Chem.* 267: 10302–10312.

Inesi G., M. Kurzmack, C. Coan, and D. E. Lewis. 1980. Cooperative calcium binding and ATPase activation in sarcoplasmic reticulum vesicles. *J. Biol. Chem.* 255:3025–3031.

James, P., M. Inui, M. Tada, M. Chiesi, E. Carafoli. 1989. Nature and site of phospholamban regulation of the Ca^{2+} pump of sarcoplasmic reticulum. *Nature.* 342:90–92.

Jones, L. R., and S. E. Cala. 1981. Biochemical evidence for functional heterogeneity of cardiac sarcoplasmic reticulum vesicles. *J. Biol. Chem.* 256:11809–11818.

Jones, L. R., H. K. Simmerman, W. W. Wilson, F. R. N. Gurd, A. D. Wegener. 1985. Purification and characterization of phospholamban from canine cardiac sarcoplasmic reticulum. *J. Biol. Chem.* 260:7721–7730.

Kinosita, K., S. Kawato, and A. Ikegami. 1977. A theory of fluorescence polarization decay in membranes. *Biophys. J.* 20:289–305.

Lewis, S. M., and D. D. Thomas. 1991. Microsecond rotational dynamics of spin-labeled Ca-ATPase during enzymatic cycling initiated by photolysis of caged ATP. *Biochemistry.* 30:8331–8339.

Lipari, G., and A. Szabo. 1980. Effect of librational motion on fluorescence depolarization and nuclear magnetic resonance relaxation in macromolecules and membranes. *Biophys. J.* 30:489–506.

Ludescher, R. D., and D. D. Thomas. 1988. Microsecond rotational dynamics of phosphorescent-labeled muscle cross-bridges. *Biochemistry.* 27:3343–3351.

Mahaney, J. E., and D. D. Thomas. 1991. Effects of melittin on molecular dynamics and Ca-ATPase activity in sarcoplasmic reticulum membranes: electron paramagnetic resonance. *Biochemistry.* 30:7171–7180.

Pethig, R., M. Kuhn, R. Payne, E. Adler, T. H. Chen, L. F. Jaffe. 1989. On the dissociation constants of BAPTA-type calcium buffers. *Cell. Calcium.* 10:491–498.

Raynor, R. L., B. Zheng, and J. F. Kuo. 1991. Membrane interactions of amphiphilic polypeptides mastoporan, melittin, polymyxin B, and cardiotoxin. *J. Biol. Chem.* 266:2753–2758.

Saffman, P. J., and M. Delbrück. 1975. Brownian motion in biological membranes. *Proc. Natl. Acad. Sci. USA.* 79:4317–4321.

Simmerman, H. K., J. H. Collins, J. L. Theibert, A. D. Wegener, L. R. Jones. 1986. Sequence analysis of phospholamban. *J. Biol. Chem.* 261:13333–13341.

Sprowl, C. D., and D. D. Thomas. 1989. Tb^{3+} luminescence and diffusion-enhanced energy transfer in DOC purified sarcoplasmic reticulum vesicles. *Biophys. J.* 55:162a.

Squier, T. C., D. J. Bigelow, and D. D. Thomas. 1988.(a). Lipid fluidity directly modulates the overall protein rotational mobility of the Ca ATPase in sarcoplasmic reticulum. *J. Biol. Chem.* 263:9178–9186.

Squier, T. C., S. E. Hughes, and D. D. Thomas. 1988.(b). Rotational dynamics and protein-protein interactions in the Ca-ATPase mechanism. *J. Biol. Chem.* 263:9162–9170.

Squier, T. C., and D. D. Thomas. 1988. Relationship between protein rotational dynamics and phosphoenzyme decomposition in the sarcoplasmic reticulum Ca-ATPase. *J. Biol. Chem.* 263:9171–9177.

Tada, M., and A. M. Katz. 1982. Phosphorylation of the sarcoplasmic reticulum and sarcolemma. *Annu. Rev. Physiol.* 44:401–423.

Teruel, J. A., and G. Inesi. 1988. Roles of phosphorylation and nucleotide binding domains in calcium transport by sarcoplasmic reticulum adenosinetriphosphatase. *Biochemistry.* 27:5885–5890.

Thomas, D. D. 1986. Rotational diffusion of membrane proteins. *In* Techniques for Analysis of Membrane Proteins. R. Cherry and I. Ragan, editors. Chapman and Hall, London. 377–431.

Thomas, D. D., and B. S. Karon. 1994. Temperature dependence of molecular dynamics and calcium ATPase activity in sarcoplasmic reticulum. *In* The Temperature Adaptation of Biological Membranes. A. R. Cossins, editor. Portland Press, London. In press.

Thomas, D. D., and J. Mahaney. 1993. The functional effects of protein and lipid dynamics in sarcoplasmic reticulum. *In* Protein-Lipid Interactions. A. Watts, editor. Elsevier Science Publishers B. V., North-Holland. 301–320.

Toyofuku, T., K. Kurzydlowski, M. Tada, and D. H. MacLennan. 1989. Identification of regions in the Ca^{2+}-ATPase of sarcoplasmic reticulum that affect functional association with phospholamban. *J. Biol. Chem.* 268:2809–2815.

Tsien, R. Y. 1980. New calcium indicators and buffers with high selectivity against magnesium and protons: design, synthesis, and properties of prototype structures. *Biochemistry.* 19:2396–2404.

Vorherr, T., M. Chiesi, R. Schwaller, and E. Carafoli. 1992. Regulation of the calcium ion pump of sarcoplasmic reticulum: reversible inhibition by phospholamban and by the calmodulin binding domain of the plasma membrane calcium ion pump. *Biochemistry.* 31:371–376.

Voss, J., D. Hussey, W. Birmachu, and D. D. Thomas. 1991. Effects of melittin on molecular dynamics and Ca-ATPase activity in sarcoplasmic reticulum membranes: time-resolved optical anisotropy. *Biochemistry.* 30:7498–7506.

Xu, Z., and M. A. Kirchberger. 1989. Modulation by polyelectrolytes of canine cardiac microsomal calcium uptake and the possible relationship to phospholamban. *J. Biol. Chem.* 264:16644–16651.